Elasticity of dense helium

Chang-Sheng Zha,[1] Ho-kwang Mao,[2] and Russell J. Hemley[2]
[1]*Cornell High Energy Synchrotron Source, Wilson Laboratory, Cornell University, Ithaca, New York 14853, USA*
[2]*Geophysical Laboratory, Carnegie Institution of Washington, 5251 Broad Branch Road, NW Washington, DC 20015, USA*
(Received 23 February 2004; revised manuscript received 11 August 2004; published 15 November 2004)

Brillouin scattering measurements have been conducted on crystals of ^{4}He at high pressure using diamond anvil cells. Complete sets of elastic moduli, aggregate sound velocities, adiabatic and isothermal equations of state, and other thermodynamic properties were obtained up to 32 GPa at room temperature. Although He adopts a hexagonal close-packed structure over the measured *P-T* range, its elasticity is close to that of a cubic material. The Cauchy condition is violated to an increasing degree with pressure and indicates an increasing role of noncentral forces such as many-body exchange interactions. The results provide detailed constraints on the density dependence of interatomic interactions and the associated lattice dynamics of this quantum solid.

DOI: 10.1103/PhysRevB.70.174107 PACS number(s): 62.20.Dc, 67.80.Cx, 78.35.+c, 64.30.+t

I. INTRODUCTION

As the second most abundant element in the cosmos, helium has been the subject of numerous scientific investigations for nearly a century. Studies in the low-*P*-*T* range have revealed the quantum and anharmonic properties of the solid phase.[1,2] As a major component of giant planets and the product of nuclear fusion, the physical properties of He at higher pressure have become a critically important issue for planetary science and astrophysics. Many experimental and theoretical investigations have been carried out to determine the crystal structure, phase diagram, equation of state, thermodynamic properties, and elasticity at high pressure.[3–18] Extensive investigations have also been done in the lower-temperature range because of its importance as a prototypical quantum system.

With the development of modern high-pressure techniques using diamond anvil cells in the last two decades, the pressure range for accurate determination of the properties of He has been greatly extended. Melting curve studies to 360 K and 16 GPa (Ref. 19) suggested a triple point at 11.6 GPa and 300 K, also studied by self-consistent phonon and Monte Carlo calculations.[20,21] Direct structure determination by high-pressure x-ray diffraction established the wide stability field of the hexagonal close-packed (hcp) phase. These measurements were extended to 58 GPa,[22] equal to the pressure range examined in shock compression experiments.[7] In addition, a number of theoretical approaches were used for modeling the behavior of dense rare gases, including helium, under extreme conditions.[19–25] None of these have been completely successful in reproducing experimental results. Discrepancies between experiments and various theoretical lattice dynamics calculations call for more extensive measurements of the physical properties of He under very high pressures.

Complete sets of elastic moduli as a function of pressure would provide important constraints on these fundamental properties for the solids. In contrast to x-ray diffraction experiments, elasticity measurements on helium at high pressures have not progressed since the early studies done in a much lower-pressure range by ultrasonic methods.[3–6,8] Ultrasonic measurements for measuring elasticity above this pressure range encountered technical difficulties, but modern diamond anvil cell techniques in conjunction with Brillouin scattering spectroscopy and synchrotron x-ray diffraction methods have proved to be very useful for these types of measurements.[26] Brillouin scattering at high pressure for helium was first carried out almost two decades ago, but no elastic moduli were obtained because the simple backscattering geometry prevents determination of the sound velocity without knowledge of the refractive index at high pressure.[27] During the last decade, developments in high-pressure Brillouin spectroscopy, including changes in diamond cell design, scattering geometry, and data collection and reduction strategies, have led to the solution of complete sets of elastic moduli for different crystal structures including solidified gases and minerals.[26,28,29] In this paper, we present a complete set of elasticity data for ^{4}He to 32 GPa at room temperature by Brillouin spectroscopy; these appear to be the first elasticity data measured for the solid in this pressure range.

II. EXPERIMENTAL TECHNIQUES

Our high-pressure Brillouin diamond-anvil cell technique[26] is described in detail elsewhere. Natural helium gas [$^4\mathrm{He}/(^3\mathrm{He}+^4\mathrm{He})=0.99986$, Air Products, Research Grade] was loaded into diamond anvil cells having a large conical opening (96°) by a high-pressure method.[30] The symmetric scattering geometry was used here for the advantage of obtaining velocities directly without knowing the refractive index of He at high pressures.[31] Multiple phonon directions were probed at each pressure and the data fit by an iterative least-squares method to invert the sound velocity data to obtain the single-crystal second-order elastic moduli (compliances C_{ij}). These compliances, and therefore the adiabatic bulk and shear moduli K_S and G, can be obtained if the density is known at the same conditions.[32] The combination of Brillouin spectroscopy and x-ray diffraction has been an effective means for determining the equations of state (EOS) and elastic properties under extreme conditions.

Helium solidifies at 11.6 GPa and 298 K.[27,33–35] In order to obtain the elastic moduli at high pressure, we need to

know the crystal structure and its density at different pressures. The first high-pressure, room-temperature, single-crystal x-ray diffraction experiments on the material confirmed that ^{4}He crystallizes in an hcp structure within the pressure range from 15.6 to 23.3 GPa (Ref. 24). Later diffraction experiments in various P-T ranges confirmed that the hcp phase persists up to 58 GPa at ambient temperature.[22] Additional room-temperature x-ray diffraction studies have been carried out more recently.[36,37]

In high-pressure research, He is considered the best hydrostatic pressure medium,[38,39] and thus we have used it extensively for studying single-crystal elasticity at high pressure. For example, He has been used as a pressure medium in the elasticity studies of α-Mg_2SiO_4, β-Mg_2SiO_4, α-$(Mg\cdot Fe)_2SiO_4$, and MgO to pressures as high as 55 GPa.[28,29,40,41] Because the incident laser beam passes through the sample and pressure medium, the scattering signals from the pressure medium are collected as a part of the spectrum under the same pressure condition. Many of the data presented in this paper are by-products of other experiments in which He was used as the pressure medium. In most situations, He was crystallized as a single crystal during the gas-loading portion of the sample preparation in order to simplify the Brillouin spectrum. This was done by very slowly clamping the anvils or through crystal growth by melting and cooling. The single crystal can be documented either by single-crystal x-ray diffraction with synchrotron radiation or by the smooth sine velocity-angle distribution measured in a crystal plane by Brillouin scattering. Furthermore, the sharp, single peak is also evidence that the material under study is a single crystal instead of a polycrystal. The latter gives rise to multiple peaks or diffuse bands as a result of the velocity anisotropy of random crystalline directions. The data used for this study corresponded to single crystals of ^{4}He. The crystal orientation was found by a fitting routine.[42,43] Finally, we point out that special attention needs to be paid to the possible pressure variation during the experiment. He is very compressible and can be difficult to stabilize at each load. As an example, a force loading that initially raises the pressure to 12.35 GPa can relax to 10.5 GPa 2 h later. The experimental details have been published previously.[28,29,40,41]

III. ELASTIC AND THERMODYNAMIC PROPERTIES

The theoretical relationship between the sound velocity, crystallographic orientation, and the elastic moduli of a hexagonal crystal has been discussed elsewhere.[26,32] The initial densities needed for evaluating the elastic moduli were obtained from the EOS determined from single-crystal x-ray diffraction.[22,36] These densities are then adjusted by thermodynamic calculations based on the obtained elastic properties. The final density and elasticity data are obtained as a self-consistent result of the iteration process described below. Explicitly, density is obtained from the thermodynamic relationship

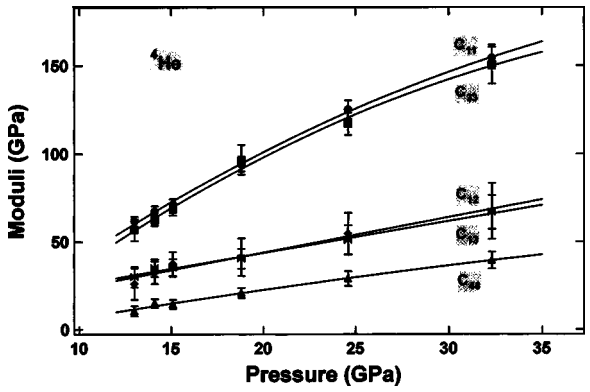

FIG. 1. The pressure dependence of single-crystal second-order elastic moduli for hcp ^{4}He.

$$\ln\left(\frac{\rho}{\rho_r}\right) = \int_{P_r}^{P} \frac{dP}{K_T}. \tag{1}$$

Here P_r and ρ_r are the reference pressure and density taken from x-ray diffraction data; this corresponds to 13.0 GPa and 0.9881 gm/cm^3 for the initial calculation.[36] Single-crystal x-ray diffractions are in good agreement in this pressure range.[22] K_T was obtained from the K_S [Eq. (9)] obtained in this study. The new densities from the integration were then used to calculate the elastic moduli; the process was repeated to reach self- consistency with respect to the bulk modulus.

The pressure dependences of the elastic moduli of ^{4}He are shown in Fig. 1 and Table I. As a hexagonal crystal, the material has five elastic moduli C_{11}, C_{33}, C_{44}, C_{12}, and C_{13}. Since there are only a few shear modes of the sound velocity that can be obtained, these provide a direct constraint for the modulus C_{12}. The expression

TABLE I. Second-order elastic moduli of ^{4}He at high pressure (300 K). Uncertainties are one standard deviation.

P (GPa)	C_{11} (GPa)	C_{33} (GPa)	C_{44} (GPa)	C_{12} (GPa)	C_{13} (GPa)
13.0	61.5(2.7)	56.7(6.2)	10.6(2.9)	26.0(9.0)	29.9(5.9)
14.1	67.3(2.9)	62.1(3.0)	15.0(2.4)	32.4(6.4)	35.0(4.9)
15.1	71.3(3.0)	68.4(3.4)	14.5(2.5)	37.4(6.8)	35.2(5.0)
18.8	93.7(3.6)	96.6(8.4)	20.9(2.8)	41.3(10.7)	40.4(5.6)
24.6	125.1(5.2)	116.9(6.4)	29.0(4.2)	54.6(11.8)	50.9(8.4)
32.3	154.2(6.2)	150.6(11.0)	39.4(4.8)	67.4(15.9)	66.7(9.6)

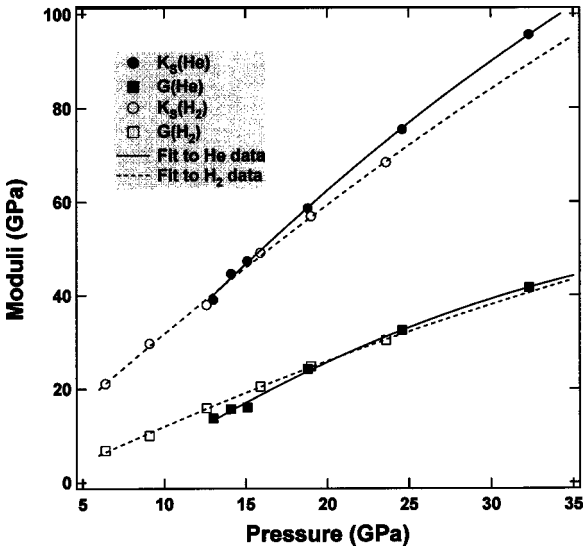

FIG. 2. Comparison of the bulk and shear moduli of ^{4}He and H_2 at different pressures.

$$C_{33} + C_{13} = C_{11} + C_{12} \tag{2}$$

has been referenced as it relates to the data fitting process.[4,26,32] Although the final results do not necessarily correspond to the expression shown above exactly, it helps to constrain and reduce the random scatter in the data for the C_{ij}. This assertion is supported by the fact that x-ray diffraction experiments demonstrate that the c/a ratio of this crystal does not change with pressure.[22,24] The data reduction algorithm is similar to that used in Ref. 26. A significant feature of the results shown in Fig. 1 is that the differences between C_{11} and C_{33} and between C_{12} and C_{13} are much smaller than the mutual uncertainties. This fact indicates that the elasticity of ^{4}He with hcp structure actually is very similar to that of a material with cubic structure, which would have only three elastic moduli C_{11}, C_{12}, and C_{44}.

Figure 2 shows the pressure dependence of the bulk and shear moduli calculated from the fitted elastic moduli. We also present our results for hydrogen for comparison. The bulk and shear moduli for ^{4}He are similar to those of H_2, in the measured range. Extrapolating to higher pressure, the shear modulus of ^{4}He shows more downwards curvature than does that of H_2. This feature could indicate that ^{4}He has lower shear strength relative to H_2 at higher pressure; this may be related to the survival of hydrogen single crystals in helium media at megabar pressures.[44] Additional insight into the comparison between these two hexagonal close-packed solids is provided by examination of the elastic anisotropy, which is determined by the individual single-crystal elastic moduli.

The elastic anisotropy for a hexagonal crystal can be described by[45]

$$\Delta p = \frac{C_{33}}{C_{11}}, \tag{3}$$

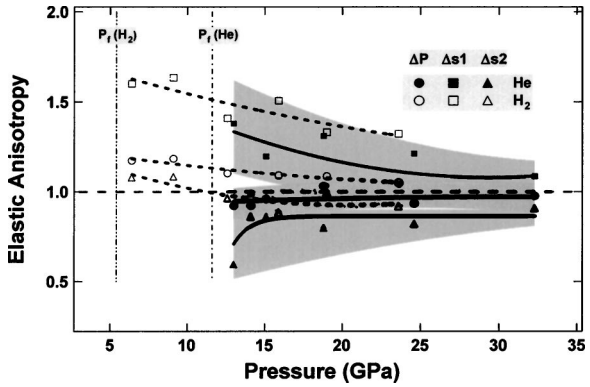

FIG. 3. The pressure tendency of the elastic anisotropy of ^{4}He and H_2. The shaded areas represent the uncertainties for each of the anisotropy determinations of ^{4}He; the uncertainties for H_2 are similar and omitted for clarification. The lines are guides to the eye. P_f(He) and $P_f(H_2)$ are the freezing pressures of helium and hydrogen, respectively, at room temperature.

$$\Delta s_1 = \frac{C_{11} + C_{33} - 2C_{13}}{4C_{44}}, \tag{4}$$

$$\Delta s_2 = \frac{C_{44}}{\frac{1}{2}(C_{11} - C_{12})}. \tag{5}$$

Here Δp, Δs_1, and Δs_2 are the anisotropies for the compressional and two shear waves, respectively, with values equal to 1 indicating elastic isotropy. Figure 3 shows the pressure dependence of the elastic anisotropy of ^{4}He from Eqs. (3)–(5). The three anisotropies are quite close to unity and do not change significantly above ~15 GPa. Figure 3 also shows the anisotropy of H_2 at high pressures. Two of the three measures of the elastic anisotropy for H_2 are higher than those of ^{4}He. Elastic anisotropy of a material is one of the sources contributing an anisotropic stress-strain response to the high-pressure environment. The difference between the two materials may be additional evidence for a more homogeneous stress-strain condition produced by ^{4}He relative to H_2 when used as a pressure-transmitting medium.

The pressure variation of the aggregate sound velocities in the fluid and solid phases are shown in Fig. 4. Polian and Grimsditch[27] measured the nv product to 20 GPa using the backscattering geometry, where n and v are the refractive index and sound velocity at a given P-T condition. Obviously, separate experiments are needed to solve for n and v. LeToullec *et al.* used an interferometric method and measured the refractive index in the fluid and solid phases,[33] and was able to successfully extract the sound velocity from the data obtained by Polian and Grimsditch. The sound velocity data for the fluid and solid phases are quite consistent with our results as shown in Fig. 4. Similar to hydrogen and in contrast to many other materials, Poisson's ratio for ^{4}He decreases with pressure over the pressure range studied (σ = 0.343–0.31 at 13–32 GPa, Table II). The change is comparable to that for hydrogen, although for a different pressure region.

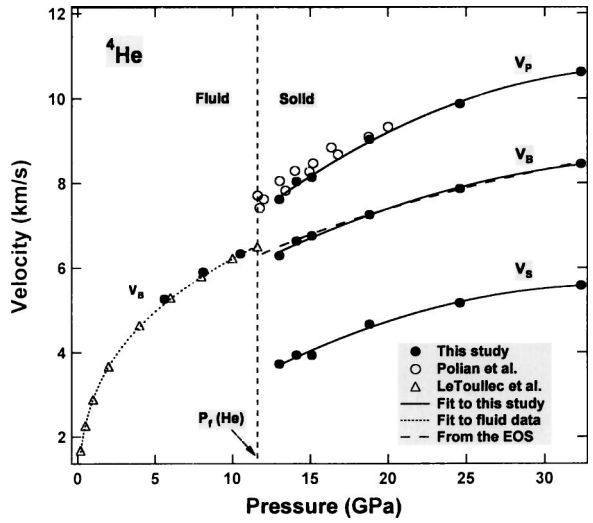

FIG. 4. Aggregate sound velocities of fluid and solid helium at high pressure and 300 K. The data from LeToullec *et al.* (Ref. 33) and Polian and Grimsditch (Ref. 27) were obtained by backscattering and a separated refractive-index measurement. Sound velocity data obtained in this study correspond to direct velocity measurements using a symmetric scattering geometry which does not require knowing the refractive index at high pressure (Ref. 31). The dashed line showing the bulk sound velocity V_B on the solid phase is calculated from the new EOS obtained in this study [see Fig. 8(a) and text]. P_f(He) is the freezing pressure of helium at room temperature.

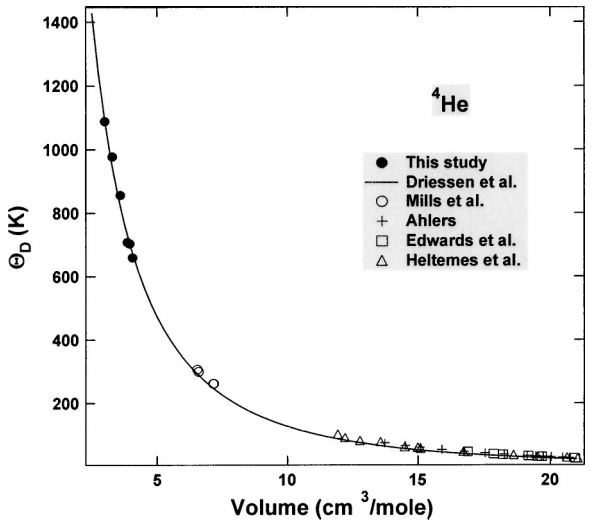

FIG. 5. The volume dependence of the Debye temperature and its comparison with previous studies. Solid line, Driessen *et al.* (Ref. 2), ○ Mills *et al.* (Ref. 6), + Ahlers (Ref. 47), □ Edwards and Pandorf (Ref. 48), and △ Heltemes and Swenson (Ref. 11).

Acoustic properties of solid He at high pressure can be used for characterizing thermodynamic states, which are not always directly measurable. The Debye model was used for determining the thermodynamic properties.[46] At each pressure, the mean velocity V_m was computed by using

$$V_m = 3^{1/3}\left(\frac{1}{V_P^3} + \frac{2}{V_S^3}\right)^{-1/3}. \tag{6}$$

The Debye temperature Θ_D and the mode-Gruneisen parameter γ can be calculated with

$$\Theta_D = h/k(3N/4\pi V_S)^{1/3} V_m, \tag{7}$$

$$\gamma = \frac{\partial \ln V_m}{\partial \ln \rho} + \frac{1}{3}, \tag{8}$$

where h is Planck's constant, k is Boltzmann's constant, and N is Avogadro's number. From the Debye temperature, the lattice specific heat at constant volume, C_V, can be obtained by integrating the Debye function. The isothermal bulk modulus K_T is calculated from the adiabatic bulk modulus K_S by

$$K_T = K_S - \rho C_V \gamma^2 T. \tag{9}$$

The ratio of specific heats at constant pressure and volume, C_P/C_V, can be written

$$C_P/C_V = K_S/K_T, \tag{10}$$

and the volumetric thermal expansion coefficient α can be calculated from

$$\alpha = \rho \gamma C_V/K_T. \tag{11}$$

Θ_D increases rapidly with pressure (Fig. 5); interestingly, it agrees well with the calculation of Driessen *et al.*,[2] which was fit to very-low-pressure data.[6,11,47,48] It is important to note that γ, C_V, C_P/C_V, and α all decrease with increasing pressure. These thermodynamic parameters are listed in Table III. LeToullec *et al.*[33] suggested a strong pressure decrease for the C_P/C_V ratio of fluid He; their value of 1.052 at 11.6 GPa is close to our result for the solid just above this pressure.

TABLE II. Aggregate elastic properties of ^{4}He at high pressure (300 K). Uncertainties are one standard deviation.

P (GPa)	ρ (g/cm^3)	K_S (GPa)	G (GPa)	σ	V_P (km/s)	V_B (km/s)	V_S (km/s)
13.0	0.9881	39.1(2.4)	13.7(1.5)	0.343	7.62(0.06)	6.29(0.05)	3.72(0.03)
14.1	1.0152	44.6(1.9)	15.7(1.2)	0.342	8.04(0.06)	6.63(0.05)	3.93(0.03)
15.1	1.0379	47.4(1.9)	16.0(1.3)	0.348	8.14(0.06)	6.76(0.05)	3.93(0.03)
18.8	1.1156	58.7(2.6)	24.2(1.7)	0.319	9.03(0.07)	7.25(0.05)	4.66(0.04)
24.6	1.2199	75.5(3.3)	32.5(2.2)	0.311	9.87(0.07)	7.86(0.06)	5.16(0.04)
32.3	1.3388	95.6(4.1)	41.6(2.7)	0.310	10.62(0.08)	8.45(0.06)	5.58(0.04)

TABLE III. Thermodynamic properties of ^{4}He at high pressure (300 K).

P (GPa)	V_m (km/s)	Θ_D (K)	γ	C_V (J/mol K)	K_T (GPa)	C_P/C_V	α (10^{-6} K^{-1})	P_{th}(0–300 K) (GPa)
13.0	4.18	659	1.61	19.9	38.7	1.01	204	1.24
14.1	4.42	703	1.60	19.3	44.3	1.01	177	1.15
15.1	4.42	707	1.60	19.2	47.0	1.01	169	1.24
18.8	5.22	856	1.58	17.1	58.3	1.01	129	0.94
24.6	5.78	977	1.56	15.5	75.1	1.00	98	0.87
32.3	6.24	1088	1.53	14.0	95.3	1.00	75	0.84

The Cauchy violation is often used to characterize the noncentral forces in classical solids at zero temperature.[23,41,49] The Cauchy relations under hydrostatic pressure conditions generally are

$$C_{12} = C_{66} + 2P,\ C_{13} = C_{55} + 2P,\ C_{23} = C_{44} + 2P. \quad (12)$$

For a crystal with hexagonal symmetry, we have[32]

$$C_{44} = C_{55},\ C_{66} = (C_{11} - C_{12})/2,\ C_{13} = C_{23}. \quad (13)$$

So Eq. (12) now gives

$$3C_{12} - C_{11} = 4P,\ \ C_{13} - C_{44} = 2P. \quad (14)$$

Figure 6 shows the pressure dependence of the Cauchy violations. As a comparison, the pressure dependences of the Cauchy violations for solid H_2 are also plotted. The relations for both materials and their pressure trends are similar, monotonically decreasing with pressure.

IV. EQUATION OF STATE

Acurate determination of the EOS of ^{4}He has been an important research objective for decades.[2,6,7,22,24,33] Based on the x-ray diffraction method developed by Mao *et al.*,[50] Loubeyre *et al.*[22] measured the lattice parameters of hcp ^{4}He to 58 GPa using synchrotron x-ray diffraction at various *P-T* conditions. Additional x-ray diffraction measurements have been conducted more recently[36,37] at room temperature. The elasticity measurements from Brillouin scattering yield the adiabatic bulk modulus as a function of pressure. The aggregate bulk (K_S) and shear (G) moduli were obtained from individual elastic moduli C_{ij} using the Voigt-Reuss-Hill averaging method[51] (Table II). Figure 7 shows the aggregate moduli as a function of density. Early measurements conducted at low pressure and low temperature are also plotted in this figure.[4,6] These data, measured decades ago by ultrasonic techniques, show good consistency with the data of the present study.

The isothermal pressure-volume relation at 300 K in this study obtained from Eq. (1) is plotted in Fig. 8(a) together with previous results.[6,10,12,14–18,52] Note that we use x-ray data only at 13 GPa. Nevertheless, the EOS determined here is quite close to recent x-ray diffraction results[36] over a wide pressure range. It is important to reduce the present data to 0 K for comparison to previous low-temperature data, particularly in the lower-pressure range. To create the EOS at 0 K, we need the thermal pressure at 300 K which then is subtracted from the measured pressure. Assuming a quasiharmonic lattice dynamical origin, the thermal pressure term (ΔP_{th}) is expressed by the Mie-Grüneisen equation[53]

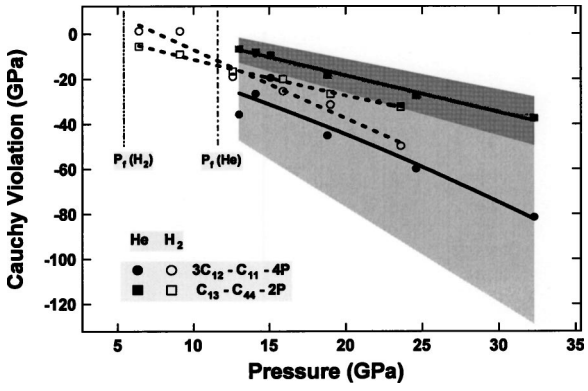

FIG. 6. The pressure dependence of the Cauchy violation in ^{4}He and H_2. The shaded areas represent the uncertainties for each of the violations of ^{4}He; the uncertainties for H_2 are similar and omitted for clarification. The solid and dashed lines are the guides to the eye. P_f(He) and P_f(H_2) are the freezing pressures of helium and hydrogen, respectively, at room temperature.

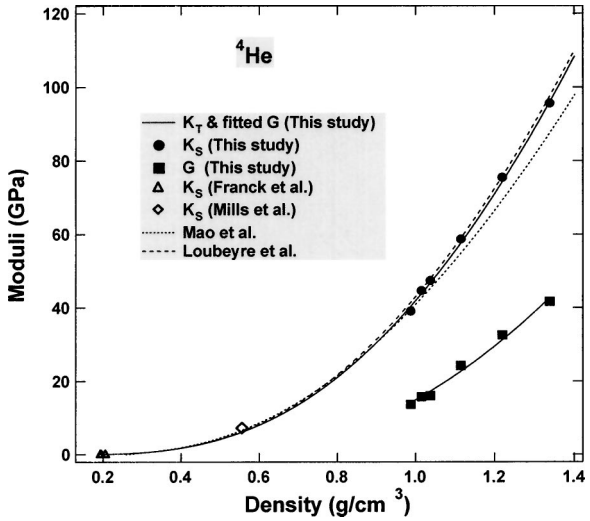

FIG. 7. Aggregate bulk moduli obtained by Brillouin scattering versus density. Several data points (△, Ref. 4; ◇, Ref. 6) at lower pressure are obtained from ultrasonic measurements and agree well with the present study.

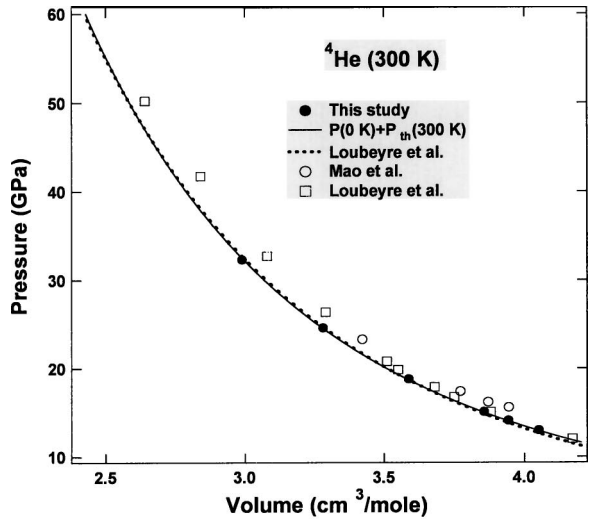

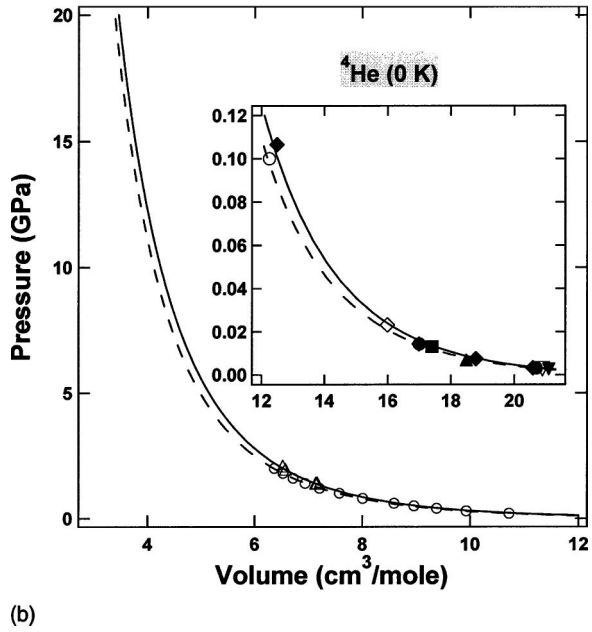

FIG. 8. (a) Equation of state of helium obtained with different experiments at room temperature. Solid line: results of the present study obtained by adding the thermal pressure at 300 K to the Vinet EOS fit of the data corrected to 0 K (see text). Dotted line: Loubeyre *et al.* (300 K, private communication). Symbols: ● this study (300 K), ○ Mao *et al.* (300 K, Ref. 24), and □ Loubeyre *et al.* (304 K, Ref. 22). (b) Equation of states of helium at low temperatures. Solid line: EOS of this study (0 K); dashed line: Driessen *et al.* (0 K, Ref. 2). Symbols: △ Mills *et al.* (75–97 K, Ref. 6), ∇ Vos *et al.* (1.3 K, Ref. 15), ◆ Vos *et al.* (1.77–14.31 K, Ref. 16), ● Mills and Schuch (1.73 K, Ref. 12), ■ Schuch and Mills (1.2–18 K, Ref. 14), ▲ Henshaw (1.1 K, Ref. 10), ▼ Minkiewicz *et al.* (1.03 K, Ref. 17), ◇ Brun *et al.* (5.6 K, Ref. 18), and ○ Stewart (4.2 K, Ref. 52).

$$\Delta P_{th} = P_{th}(V,T) - P_{th}(V,T_0) = [\gamma(V)/V][E_{th}(V,T) - E_{th}(V,T_0)], \quad (15)$$

where the subscript 0 refers to 0 K. The Grüneisen parameter γ, assumed to be independent of temperature but volume dependent, has been calculated above. The internal energy term E_{th} can be evaluated in terms of the Debye function

$$E_{th} = \frac{9nRT^4}{\Theta_D{}^3}\int_0^{x_D}\frac{x^3}{e^x-1}dx, \quad (16)$$

$$\Delta P_{th} = \frac{9n\gamma(V)RT^4}{V\Theta_D{}^3}\int_0^{x_D}\frac{x^3}{e^x-1}dx, \quad (17)$$

where n is the number of atoms per formula unit, R is the gas constant, and $x_D=\Theta_D/T$. The calculated P_{th} are listed in Table III. The thermal pressure P_{th} was subtracted from each measured pressure to obtain the pressure at 0 K for each volume at 300 K. It is well known that the choice of zero-pressure reference volume V_0 will strongly affect the final EOS parameters; this cannot be measured directly for hcp ^{4}He at any temperature. Stewart[52] measured the compression of solid ^{4}He using the piston displacement method at 4.2 K up to 2 GPa. Edwards and Pandorf[48] measured the heat capacity of hcp ^{4}He at 0.3–4.27 K and obtained a set of thermodynamic properties at 0 K including the *P-V-T* relationship. Other experimental studies of the density and structure have been carried out at low temperatures and pressures, including x-ray diffraction,[10,13,14] neutron scattering,[17] and thermodynamic measurements.[54] The Vinet *P-V* function was used to fit all of these data, and $V_0=25.35$ cm^3/mol at 0 K was obtained; the small temperature differences within those data have a negligible effect on the result. This value for V_0 was then used in a Vinet EOS fit of the present higher-pressure data corrected to 0 K giving $K_{0\,T}=0.0064(\pm0.0003)$ GPa, and $K'_{0\,T}=9.71(\pm0.06)$. The consistency between the EOS and previous work [including the results of Driessen *et al.*;[2] see Fig. 8(b)] is very good over a wide pressure range.

V. DISCUSSION

We have presented a complete set of elastic moduli for solid ^{4}He up to 32 GPa at room temperature, measured by Brillouin scattering spectroscopy. We found that this hcp crystal has an elasticity rather similar to that of a cubic material with $C_{11}\approx C_{33}$ and $C_{12}\approx C_{13}$, within experimental uncertainties. The almost isotropic elastic properties and possibly softer shear modulus at higher pressure are also consistent with its better hydrostatic character relative to hydrogen. The pressure-volume relation based on an iterative calculation using the elasticity data fit to a Vinet EOS is consistent with the results of x-ray diffraction measurements. Indeed, we find that the Vinet EOS function is capable of fitting *P-V* data over a very broad range of compression, as found previously for H_2.[55] The new elasticity data obtained over the large compression range provide an opportunity for assessing the origin of discrepancies between lattice dynamical calculations based on different interatomic potential models and experimental measurements.

As mentioned above, extensive theoretical lattice dynamics calculations and simulations have been carried out on He over a range of densities.[1] These include self-consistent phonon calculations,[21,56,57] in which the phonon frequencies and elastic constants as well as the free energies and therefore the EOS are determined. First-order self-consistent phonon approximations have been used but primarily for examining the properties of the low-pressure solid.[1] During the past few decades, static and dynamic compression experiments have provided experimental data over much larger pressure-temperature ranges. Lattice dynamics calculations of the EOS (Refs. 22 and 24) based on accurate pure pair potentials[58,59] produce much higher pressures relative to experiment; i.e., there is a significant softening due to attractive many-body interactions. Similar results were found for Ne.[60,61] Calculations based on the Ross-Young potential for He,[62] which is an exponential-6 type obtained from fitting to shock-wave data and implicitly including many-body terms, are more consistent with experimental data but tend to disagree in the higher-pressure range. On the other hand, self-consistent harmonic phonon calculations corrected with three-body interaction terms[20] give a much softer EOS than obtained with the experimental data.[22] Recently, the path-integral Monte Carlo simulations method has successfully been used to reproduce the room-temperature EOS of Ne,[63] but apparently has not been applied to dense He (see also Ref. 60).

Elasticity data obtained over a large pressure range provide detailed constraints on the explicit form of the interatomic interactions in the dense solid. The degree of the Cauchy violation in this quantum solid thus provides additional information that may be compared with violations observed previously in classical solids.[23,41] The Cauchy violation at low pressure can be ascribed to quantum fluctuations and the strongly anharmonic dynamics of the system (Fig. 6). The lattice dynamics of rare-gas solids become increasingly harmonic under pressure.[60] The pressure dependence of the Cauchy violation indicates the increasing role of many-body (noncentral) forces with density, consistent with analyses of the EOS of other rare-gas solids. In this regard, comparison between the ^{4}He and H_2 is also instructive. Both have similar bulk elastic properties; the Cauchy relations and elastic anisotropies, which depend on the individual elastic moduli, differ but the trends with pressure are similar. The electron density of solid molecular hydrogen is close to spherical in this pressure range (well below orientational ordering transitions), despite the differences in the underlying atomic structure (monoatomic versus diatomic in this P-T range). The magnitude of the differences in elasticity properties between ^{4}He and H_2 at high density should provide important tests of theory. In addition to identifying the explicit form and magnitude of the interatomic interactions, calculations of the elasticity that include the density dependence of the quantum properties are needed to examine these issues. As such, Brillouin measurements on these and related simple molecular systems over a wider pressure range would be useful.

ACKNOWLEDGMENTS

We thank T. S. Duffy, R. T. Downs, and J. Hu for their valuable help in these experiments, P. Loubeyre for sharing his unpublished EOS data, Yu. A. Freiman for many useful discussions, and S. Gramsch for comments on the manuscript. C.S.Z. is supported by CHESS through a NSF grant and NIH/NIGMS under Award No. DMR 0225180. H.K.M. and R.J.H. are supported by NSF-DMR, NASA, and DOE/NNSA through the Carnegie/DOE Alliance Center (CDAC, DOE Contract No. DE-FC03-03NA00144).

[1] M. L. Klein and T. R. Koehler, in *Rare Gas Solids*, edited by M. L. Klein and J. A. Venables (Academic Press, London, 1976), Vol. 1, p. 301.
[2] A. Driessen, E. van der Poll, and I. F. Silvera, Phys. Rev. B **33**, 3269 (1986).
[3] R. H. Crepeau, O. Heybey, D. M. Lee, and S. A. Strauss, Phys. Rev. A **3**, 1162 (1971).
[4] J. P. Franck and R. Wanner, Phys. Rev. Lett. **25**, 345 (1970).
[5] F. P. Lipschultz and D. M. Lee, Phys. Rev. Lett. **14**, 1017 (1965).
[6] R. L. Mills, D. H. Liebenberg, and J. C. Bronson, Phys. Rev. B **21**, 5137 (1980).
[7] W. J. Nellis, N. C. Holmes, A. C. Mitchell, R. J. Trainor, G. K. Governo, M. Ross, and D. A. Young, Phys. Rev. Lett. **53**, 1248 (1984).
[8] J. H. Vignos and H. A. Fairbank, Phys. Rev. **147**, 185 (1966).
[9] R. Wanner and J. P. Franck, Phys. Rev. Lett. **24**, 365 (1970).
[10] D. G. Henshaw, Phys. Rev. **109**, 328 (1958).
[11] E. C. Heltemes and C. A. Swenson, Phys. Rev. **128**, 1512 (1962).
[12] R. L. Mills and A. F. Schuch, in *Proceedings of the Eighth International Conference on Low-Temperature Physics, London, 1962*, edited by R. O. Davies (Butterworths, London, 1963), p. 423.
[13] A. F. Schuch and R. L. Mills, Phys. Rev. Lett. **8**, 469 (1962).
[14] A. F. Schuch and R. L. Mills, Acta Crystallogr. **16**, A20 (1963).
[15] J. E. Vos, B. S. Blaisse, D. A. E. Boon, W. J. V. Scherpenzeel, and R. Kingma, Physica (Amsterdam) **37**, 51 (1967).
[16] J. E. Vos, R. V. Kingma, F. J. Van der gaag, and B. S. Blaisse, Phys. Lett. **24A**, 738 (1967).
[17] V. J. Minkiewicz, T. A. Kitchens, F. P. Lipschultz, R. Nathans, and G. Shirane, Phys. Rev. **174**, 267 (1968).
[18] T. O. Brun, S. K. Sinha, C. A. Swenson, and C. R. Tilford, in *Proceedings of the Symposium on Neutron Inelastic Scattering, Copenhagen, Denmark, 1968* (International Atomic Energy Agency, Viena, Austria, 1968), Vol. 1, p. 339.
[19] P. Loubeyre, J. M. Besson, J. P. Pinceaux, and J. P. Hansen, Phys. Rev. Lett. **49**, 1172 (1982).
[20] P. Loubeyre, Phys. Rev. Lett. **58**, 1857 (1987).
[21] P. Loubeyre, D. Levesque, and J. J. Weis, Phys. Rev. B **33**, 318 (1986).
[22] P. Loubeyre, R. LeToullec, J. P. Pinceaux, H. K. Mao, J. Hu, and R. J. Hemley, Phys. Rev. Lett. **71**, 2272 (1993).
[23] M. Grimsditch, P. Loubeyre, and A. Polian, Phys. Rev. B **33**, 7192 (1986).
[24] H. K. Mao, R. J. Hemley, Y. Wu, A. P. Jephcoat, L. W. Finger, C.

S. Zha, and W. A. Bassett, Phys. Rev. Lett. **60**, 2649 (1988).
[25] D. A. Young, A. K. McMahan, and M. Ross, Phys. Rev. B **24**, 5119 (1981).
[26] C. S. Zha, T. S. Duffy, H. K. Mao, and R. J. Hemley, Phys. Rev. B **48**, 9246 (1993).
[27] A. Polian and M. Grimsditch, Europhys. Lett. **2**, 849 (1986).
[28] C. S. Zha, T. S. Duffy, R. T. Downs, H. K. Mao, and R. J. Hemley, J. Geophys. Res. **101**, 17 535 (1996).
[29] C. S. Zha, T. S. Duffy, H. K. Mao, R. T. Downs, R. J. Hemley, and D. J. Weidner, Earth Planet. Sci. Lett. **147**, E9 (1997).
[30] R. L. Mills, D. H. Liebenberg, J. C. Bronson, and L. C. Schmidt, Rev. Sci. Instrum. **51**, 891 (1980).
[31] C. H. Whitfield, E. M. Brody, and W. A. Bassett, Rev. Sci. Instrum. **47**, 942 (1976).
[32] M. J. P. Musgrave, *Crystal Acoustics* (Holden-Day, San Francisco, 1970).
[33] R. L. Toullec, P. Loubeyre, and J.-P. Pinceaux, Phys. Rev. B **40**, 2368 (1989).
[34] P. Loubeyre, R. L. Toullec, and J.-P. Pinceaux, Phys. Rev. Lett. **70**, 2106 (1993).
[35] F. Datchi, P. Loubeyre, and R. LeToullec, Phys. Rev. B **61**, 6535 (2000).
[36] P. Loubeyre (private communication).
[37] P. Loubeyre, R. LeToullec, M. Hanfland, L. Ulivi, F. Datchi, and D. Hausermann, Phys. Rev. B **57**, 10 403 (1998).
[38] P. M. Bell and H. K. Mao, Year Book - Carnegie Inst. Washington **80**, 404 (1981).
[39] R. T. Downs, C. S. Zha, T. S. Duffy, and L. W. Finger, Am. Mineral. **81**, 51 (1996).
[40] C. S. Zha, T. S. Duffy, R. T. Downs, H. K. Mao, and R. J. Hemley, Earth Planet. Sci. Lett. **159**, 25 (1998).
[41] C. S. Zha, H. K. Mao, and R. J. Hemley, Proc. Natl. Acad. Sci. U.S.A. **97**, 13 494 (2000).
[42] H. Shimizu and S. Sasaki, Science **257**, 514 (1992).
[43] S. V. Sinogeikin and J. D. Bass, Phys. Rev. B **59**, R14 141 (1999).
[44] P. Loubeyre, R. LeToullec, D. Hausermann, M. Hanfland, R. J. Hemley, H. K. Mao, and L. W. Finger, Nature (London) **383**, 702 (1996).
[45] G. Steinle-Neumann, L. Stixrude, and R. E. Cohen, Phys. Rev. B **60**, 791 (1999).
[46] M. Born and K. Huang, *Dynamical Theory of Crystal Lattices* (Clarendon, Oxford, 1954).
[47] G. Ahlers, Phys. Rev. A **2**, 1505 (1970).
[48] D. O. Edwards and R. C. Pandorf, Phys. Rev. **140**, A816 (1965).
[49] V. V. Brazhkin and A. G. Lyapin, Phys. Rev. Lett. **78**, 2493 (1997).
[50] H. K. Mao, A. P. Jephcoat, R. J. Hemley, L. W. Finger, C. S. Zha, R. M. Hazen, and D. E. Cox, Science **239**, 1131 (1988).
[51] J. P. Watt and L. Peselnick, J. Appl. Phys. **51**, 1525 (1980).
[52] J. W. Stewart, Phys. Rev. **129**, 1950 (1963).
[53] E. Grüneisen, Hanb. Phys. **10**, 1 (1926).
[54] C. A. Swenson, Phys. Rev. **79**, 626 (1950).
[55] R. J. Hemley, H. K. Mao, L. W. Finger, A. P. Jephcoat, R. M. Hazen, and C. S. Zha, Phys. Rev. B **42**, 6458 (1990).
[56] N. R. Werthamer, *Self-consistent Phonon Theory of Rare Gas Solids* (Academic Press, London, 1976), Vol. 1, p. 265.
[57] H. R. Glyde and V. V. Goldman, J. Low Temp. Phys. **25**, 601 (1976).
[58] R. A. Aziz, V. P. S. Nain, J. S. Carley, W. L. Taylor, and G. T. McConville, J. Chem. Phys. **70**, 4330 (1979).
[59] R. A. Aziz, F. R. W. McCourt, and C. C. K. Wong, Mol. Phys. **61**, 1487 (1987).
[60] R. J. Hemley, C. S. Zha, A. P. Jephcoat, H. K. Mao, L. W. Finger, and D. E. Cox, Phys. Rev. B **39**, 11 820 (1989).
[61] R. J. Hemley and H. K. Mao, J. Low Temp. Phys. **122**, 331 (2001).
[62] M. Ross and D. A. Young, Phys. Lett. A **118**, 463 (1986).
[63] M. Neumann and M. Zoppi, Phys. Rev. B **62**, 41 (2000).